PCCP

PAPER

View Article Online
View Journal | View Issue

Cite this: *Phys. Chem. Chem. Phys.*, 2014, **16**, 9096

Combined transparency and optical nonlinearity enhancement in flexible covalent multimers by operating through-space interactions between dipolar chromophores†

Venkatakrishnan Parthasarathy,[ab] Ravindra Pandey,[c] Francesca Terenziani,*[d] Puspendu K. Das*[c] and Mireille Blanchard-Desce*[ae]

Received 18th February 2014,
Accepted 17th March 2014

DOI: 10.1039/c4cp00715h

www.rsc.org/pccp

Subtle manipulation of mutual repulsion and polarisation effects between polar and polarisable chromophores forced in closed proximity allows achieving major (100%) enhancement of the first hyperpolarisability together with increased transparency, breaking the well-known nonlinearity–transparency trade-off paradigm.

1 Introduction

Efficient organic materials for nonlinear optics (NLO) are in high demand. Obtaining electro-optic organic materials with excellent second-order susceptibility, $\chi^{(2)}$, is still a vibrant area of research, due to their promising applications in telecommunication, optical computation, second harmonic generation (SHG) and THz wave generation, to name a few.[1–7]

Among various chromophores, push–pull polyenes have been demonstrated to show very large first hyperpolarisability (β) which can be enhanced by increasing the polyenic chain length[8–13] and using suitable donor (D) and acceptor (A) end groups in order to achieve optimum bond length alternation (BLA)[8,14,15] and ground-state intramolecular charge transfer (ICT).[10,15–19] The main disadvantage associated with such highly polarizable long π-conjugated systems is that they possess an intense and broad absorption band at long wavelengths (thus compromising transparency)[8,9,12,14] and often a discouraging (photo)chemical stability.[12,15,20]

Recently we have shown that molecular engineering of intramolecular interactions in multimers of dipolar and polarizable compounds could lead to enhancement (by about 30%) of third-order NLO responses (namely two-photon absorption) while increasing the transparency.[20] Such achievement is even more challenging when dealing with second-order NLO responses because of the strong constraints related to symmetry. The close proximity between dipolar chromophores with large dipole moments generally favours their arrangement in an anti-parallel fashion and the formation of dimers or aggregates,[21–23] leading to a marked decrease in the quadratic NLO overall response. This is the reason why dipolar interactions are usually considered deleterious for second-order effects and motivated numerous elegant approaches for obtaining large $\chi^{(2)}$ values by preventing, decreasing or counterbalancing dipole–dipole interactions.[1,24–27]

We herein describe a different route where push–pull chromophores are gathered in close proximity by covalent linking. Compared to the seminal innovative work by Reinhoudt and coworkers and others,[28–33] we focused on strongly *dipolar and polarizable* chromophores and did not use a large platform (such as cyclodextrins or calixarenes) but very short methylenic (*non-conjugated*) spacers in order to enhance dipolar interactions between chromophores. Our aim is to take advantage of self-orientation (driven by dipolar repulsion) and mutual polarisation effects (*i.e. through-space* electrostatic interactions) to modulate their ground-state polarity and (hyper)polarisability towards the optimum values (Fig. 1). A particular emphasis will be made on increasing both the NLO responses and the transparency. Following this aim, we report the major enhancement of the first hyperpolarisability, β (both overall and per subunit), for a set of *ad hoc* designed dimeric architectures (Scheme 1).

[a] *Chimie et Photonique Moléculaires (CNRS UMR 6510), Université de Rennes 1, 35042 Rennes, France*
[b] *Department of Chemistry, Indian Institute of Technology Madras, Chennai–600 036, India*
[c] *Department of Inorganic and Physical Chemistry, Indian Institute of Science (IISc), Bangalore 560012, India. E-mail: pkdas@ipc.iisc.ernet.in; Tel: +91 80 22 93 26 62*
[d] *Dipartimento di Chimica & INSTM UdR-Parma, Università di Parma, 43124 Parma, Italy. E-mail: francesca.terenziani@unipr.it; Tel: +39 0521 905453*
[e] *Institut des Sciences Moléculaires (CNRS UMR 5255), Université de Bordeaux, 33400 Talence, France. E-mail: mireille.blanchard-desce@u-bordeaux.fr; Tel: +33 (0)5 40 00 67 32*

† Electronic supplementary information (ESI) available: Full description of synthetic details and characterization; further details on HRS; the two-level model for push–pull chromophores. See DOI: 10.1039/c4cp00715h

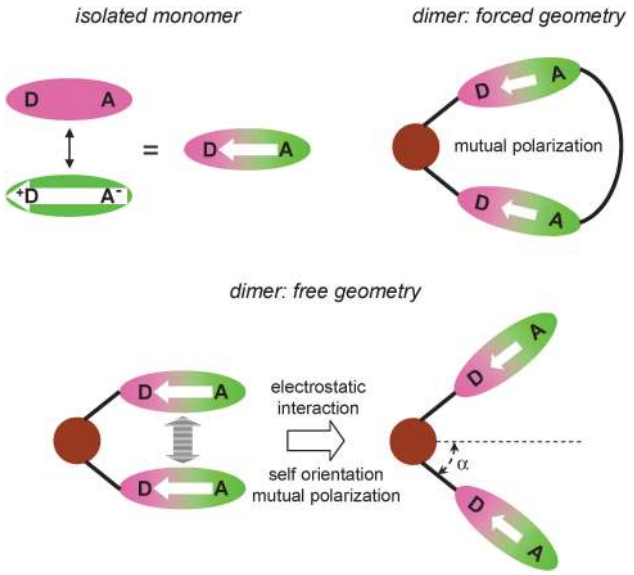

Fig. 1 Cartoon diagram representing the implemented approach. The monomer is represented by its two resonating structures (neutral and zwitterionic), and by its resulting ICT ground state. The cyclic dimer is represented with its forced geometry. The free dimers are represented by showing the electrostatic interactions between the subunits, responsible for self-orientation and mutual polarisation of the two subchromophores. The white arrows represent the dipole moments of the subchromophores: by the effect of mutual polarisation, repulsive interactions are responsible for a decrease of the dipole moment of the subunits (shorter arrows in the cartoon).

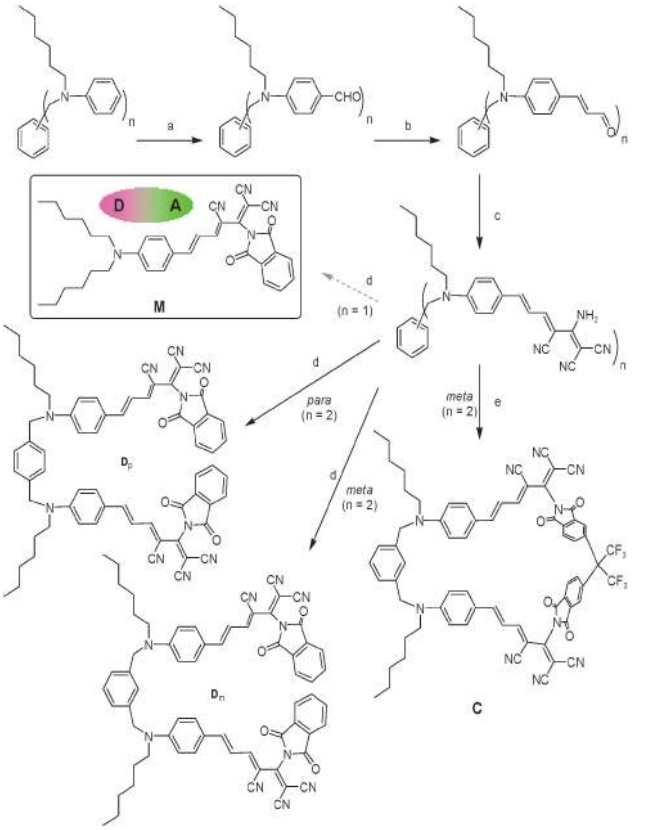

Scheme 1 Synthesis of model monomer and dimers. *Reagents and conditions*: (a) $POCl_3$, dry DMF, 5 °C – rt, 1 h, then rt –90 °C, 4 h, 84–94%; (b) tributyl-[1,3]-dioxolan-2-ylmethylphosphonium bromide, NaH, dry THF, rt, 12 h, then 1 N HCl, 83–95%; (c) 2-amino-1,1,3-tricyano-1-propene, anhy. EtOH, reflux, 24–48 h, 79–85%; (d) phthalic anhydride, Et_3N, CH_2Cl_2, reflux, 4 h, 40–60%; (e) 4,4′-(hexafluoroisopropylidene)bisphthalic anhydride, Et_3N, CH_2Cl_2, reflux, 0.5 h, 13%.

2 Experimental methods

2.1 Synthesis

All reactions involving air- or water-sensitive compounds were carried out under argon. Solvents were generally dried and distilled prior to use. Reactions were monitored by TLC on Merck 60 F254 aluminum sheets precoated with silica gel. Column chromatography was performed using Merck silica gel Si 60 (40–63 mm, 230–400 mesh), unless otherwise noted. IR spectra were recorded on a Perkin Elmer Spectrum 100 FT-IR spectrometer with solid samples. NMR studies were carried out using a Bruker ARX 200 (^{1}H: 200.13 MHz, ^{13}C: 50.32 MHz) or a Bruker Biospin (^{1}H: 300.13 MHz, ^{13}C: 75.47 MHz) High Performance Digital FTNMR Spectrometer, in $CDCl_3$ solutions; ^{1}H chemical shifts are given in ppm relative to TMS as the internal standard, J values in Hz, and ^{13}C chemical shifts relative to the central peak of $CDCl_3$ at 77.0 ppm. NMR studies were conducted using 10^{-2}–10^{-3} M solution in $CDCl_3$. High-resolution mass spectra were recorded at the Centre Régional de Mesures Physiques de l'Ouest (C.R.M.P.O., Rennes), using a Micromass MS/MS ZABSpec TOF instrument with EBE TOF geometry; liquid secondary ion mass spectrometry (LSI-MS) was performed at 8 kV with Cs^+ in *m*-nitrobenzyl alcohol (*m*NBA). Melting points reported are uncorrected. All the compounds were characterized and analyzed by infra-red spectroscopy (IR), Nuclear Magnetic Resonance spectroscopy (NMR), UV–vis spectroscopy, HRS, HRMS and microanalysis. The starting materials, such as *N*-hexylaniline,[34] *N*,*N*-di-*n*-hexylaniline,[35] tributyl-[1,3]-dioxolan-2-ylmethylphosphonium bromide[36] and 2-amino-1,1,3-tricyano-1-propene,[37] were prepared according to the procedures reported in the literature. Commercial compounds, such as phthalic anhydride, 4,4′-(hexafluoroisopropylidene)-bisphthalic anhydride and triethylamine, purchased were used as such. The detailed synthesis and characterization of the multichromophores is reported in the ESI.†

2.2 Photophysical characterization

UV-Vis spectra were recorded on a Jasco V-570 spectrophotometer for about 10^{-5} M solutions. The molar extinction coefficients were derived from the slope of the absorbance *versus* concentration graphs resulting from solutions obtained from independent weighing, and were checked for Beer–Lambert's law. Solvents used were of spectroscopic grade. All measurements were carried out at room temperature.

The first hyperpolarisabilities of the compounds were measured at 1907 nm (fundamental wavelength) in solution by the hyper-Rayleigh scattering technique. A light beam at 1907 nm was generated as the 1st Stokes line of 1064 nm by stimulated Raman scattering (SRS) in hydrogen gas.[38,39] The fundamental laser beam at 1064 nm from a Nd:YAG laser was allowed to pass through a cylindrical cell filled with 99.9% pure hydrogen gas at 50 kg cm^{-2}.

The 1907 nm beam was separated from other wavelengths using a long-pass filter and a dichroic mirror which rejected the unconverted incident light. The energy of the incident laser beam on the Raman-shifter cell was kept below 450 mJ pulse^{-1} to suppress other nonlinear optical processes such as self-focusing and Brillouin scattering. The 1907 nm beam was focused into a cylindrical sample cell of 20 mL volume, using a plano-convex lens of focal length 200 mm. The energy of the incident 1907 nm beam was maintained in the range of 13–18 mJ pulse^{-1}. Second harmonic scattered light at 953.5 nm from the sample was collected at a right angle on a photomultiplier tube (Hamamatsu R5108), using a bi-convex aspheric lens (diameter = 40 mm, focal length = 29.5 mm), a band pass filter of bandwidth 950 ± 11 nm, and a cut-off filter of 1907 nm. The output from the photomultiplier tube was amplified 5 times, averaged over 500 shots and recorded using a digital storage oscilloscope (Tektronix TDS 3052B) and processed in a PC. The set-up for the HRS experiment at 1907 nm is shown in the ESI,† Fig. S2. More details of the experimental set up are available elsewhere.[40]

The hyperpolarisability of the compounds was determined using the external reference method.[41,42] In this method, the SHG signal from an unknown sample is measured relative to that of a reference sample. Here DR1 (Disperse Red 1) was used as the reference molecule for all the measurements performed at 1907 nm.[43] The hyperpolarisability of DR1 is taken as 22.7 × 10^{-30} esu in chloroform. It is calculated by using $\beta_{HRS} = \sqrt{6/35}\beta_{EFISHG}$, from the reported EFISHG β value ($\beta_{EFISHG} = \beta_{111} = 55 \times 10^{-30}$ esu).[44] The reported hyperpolarisabilities are given in the X convention as defined in ref. 45. The power dependence study was carried out to check the quadratic incident power dependence of the HRS signal. Solute concentrations were kept in the range of 10^{-6}–10^{-5} M for all measurements.

3 Theoretical methods

3.1 Theoretical model for interacting chromophores

The excitonic Hamiltonian describing two interacting two-level chromophores can be written as follows:[46]

$$H_{exc} = \hbar\omega_{ge}(\hat{n}_1 + \hat{n}_2) + J(\hat{b}_1\hat{b}_2^{+} + \hat{b}_2^{+}\hat{b}_1) \quad (1)$$

where $\hbar\omega_{ge}$ is the excitation energy of the single subunit; indexes 1 and 2 represent the two chromophoric subunits; $\hat{n}_i$ is the operator counting excitations on the i-th subunit; $\hat{b}_i(\hat{b}_i^{+})$ is the operator which destroys (creates) one exciton on the i-th site; J is the exciton hopping term between the two chromophores (which is proportional to the squared transition dipole moment of the interacting chromophores), and depends on the interchromophore distance and relative orientation (d and α, see below). The interaction responsible for exciton hopping has been screened using the squared refractive index of the solvent.

The complete Hamiltonian describing all terms stemming from electrostatic interchromophoric interactions (detailed in ref. 47) would contain other contributions, namely the exciton–exciton interaction term, and some other terms mixing states having different exciton numbers. We verified that these contributions are negligible when calculating linear responses (like absorption spectra), but sizable for nonlinear responses. The Hamiltonian in eqn (1) formally corresponds to the standard Frenkel exciton Hamiltonian. The only difference with respect to the standard implementation is in the evaluation of the excitation energy, $\hbar\omega_{ge}$: while in the standard treatment this is fixed to the value relevant to the isolated chromophore, in our approach $\hbar\omega_{ge}$ is relevant to the *interacting* subunit, *i.e.* it differs from the value for the isolated reference chromophore because the presence of the other chromophore at a close distance induces changes in the molecular properties due to the molecular polarisability. This effect is self-consistent and can be well estimated through a mean-field calculation.[47]

In the calculations of the spectra, a Gaussian lineshape is assigned to each transition, arbitrarily imposing a half-width at half-maximum of 0.1 eV. Calculated spectra and properties are not aimed at reproducing all features of the experimental ones, but only at giving clues on the relative intensities of the linear and nonlinear processes when comparing the dimers to the reference chromophore.

3.2 First hyperpolarisability for a dimer having C_{2v} symmetry: vector analysis

The first hyperpolarisability for a dimer composed of two push–pull chromophores can be expressed as a function of the hyperpolarisability of the single subunit, β_{zzz}(**sub**). Each push–pull subunit can be approximated as having a major component of its first hyperpolarisability along its molecular axis (z). For a dimer of C_{2v} symmetry, the β_{HRS} response can be expressed as follows:[48]

$$\langle\beta_{HRS}^2\rangle = 4\left[\frac{6}{35}\cos^6\alpha + \frac{16}{105}\cos^4\alpha\sin^2\alpha + \frac{38}{105}\cos^2\alpha\sin^4\alpha\right]$$

$$\beta_{zzz}^2(\mathbf{sub}) = 4\left[\cos^6\alpha + \frac{8}{9}\cos^4\alpha\sin^2\alpha + \frac{19}{9}\cos^2\alpha\sin^4\alpha\right] \quad (2)$$

$$\langle\beta_{HRS}^2\rangle^{(\mathbf{sub})} = 4[F(\alpha)]^2\langle\beta_{HRS}^2(\mathbf{sub})\rangle$$

where β_{zzz}(**sub**) can be different from the β_{zzz} of the monomeric model, *i.e.* β_{zzz}(**M**), because of the mutual polarisation of the chromophores in the dimer. The $F(\alpha)$ function is reported as a graph in Fig. 2. If β_{zzz}(**sub**) would coincide with the β_{zzz} of the monomeric model, the β^{HRS}(**dimer**)/[$2\beta^{HRS}$(**M**)] ratio could not exceed 1. The observation of ratios of about 1.5 (see Table 1) is a clear demonstration that the hyperpolarisability of the subunit, β_{zzz}(**sub**), is much bigger than that of the isolated chromophore.

4 Results and discussion

A push–pull chromophore (**M**) of definite length bearing suitable strong donor and acceptor end groups to ensure significant ground-state ICT and large polarisability was chosen; the small and rigid benzene core in multi **M**-chromophores was opted to ensure close proximity between the subchromophores, as well as different substitution patterns (*meta* and *para*) to control the interchromophoric distance and the extent of interactions

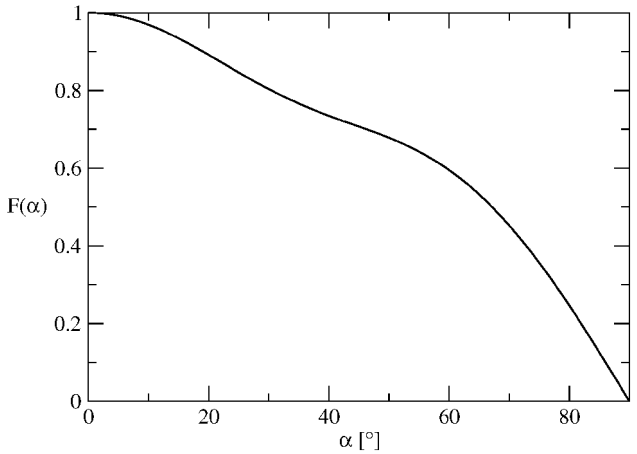

Fig. 2 The $F(\alpha)$ function describing the dependence of the first hyperpolarisability of a C_{2v} dimer with respect to that of the subchromophores (see eqn (2)).

Table 1 ^{1}H NMR, absorption and HRS data of monomeric and dimeric derivatives in chloroform

	M	$\mathbf{D}_p$	$\mathbf{D}_m$	**C**
N	1	2	2	2
$\Delta J = J_{12} - J_{23}$ [Hz][a]	2.1	2.55	2.7	2.6
λ_{max} [nm]	670	651	648	630
ε_{max} [10^4 M^{-1} cm^{-1}]	10.6	12.4	12.7	10.8
β^{HRS} [10^{-30} esu]	56	164	155	135
β_0^{HRS} [10^{-30} esu][b]	25	77	74	68
$\beta^{HRS}/\beta^{HRS}(\mathbf{M})$	1	2.9	2.8	2.4
$\beta_0^{HRS}/(N\beta_0^{HRS}(\mathbf{M}))$	1	1.5	1.5	1.4
$\beta_{zzz}(\mathbf{sub})/\beta_{zzz}(\mathbf{M})$	1	2.3	2.2	1.8

[a] Measured in $CDCl_3$; numbering from donor to acceptor end groups; average difference in $^3J_{HH}$ values across adjacent C=C and C–C bonds. [b] Static hyperpolarisability β_0^{HRS} was extrapolated by using the relation $\beta_0^{HRS} = \beta^{HRS}/f$; frequency factor, $f = (1 - (\lambda_{max}^2/\lambda_{HRS}^2))(1 - 4(\lambda_{max}^2/\lambda_{HRS}^2))$.

within the covalent architecture; short and flexible methylenic linkers were used to allow self-orientation while retaining close proximity. Accordingly, the model monomer and the related dimers were prepared in moderate to reasonable yields as described in Scheme 1 (for procedures and characterization details, see ESI†). The series also includes a non-conjugated macrocycle **C** where the parallel relative orientation of chromophoric subunits is imposed. We observe a significant variation in synthetic yield depending on the nature of the end-groups and proximity of polar chromophoric subunits. For instance, the condensation of 2-amino-1,1,3-tricyano-1-propene with aldehyde **3M**, **3D**$_p$ and **3D**$_m$ (see Scheme S1, ESI†) shown in step c in Scheme 1 gives similar yields for the monomer and dimers (79–85%), with dimers requiring longer reaction times (typically 60 h instead of 8 h). The reaction of **4M**, **4D**$_p$ and **4D**$_m$ (see Scheme S1, ESI†) with phthalic anhydride (step d in Scheme 1) yields final compounds (**M**, $\mathbf{D}_p$ and $\mathbf{D}_m$) which bear much stronger end-groups and consequently are more polar. Interestingly, the condensation proceeds with much lower yields for dimers (40 and 60%) compared to the monomer (83%). This is a clear indication that strong dipole–dipole

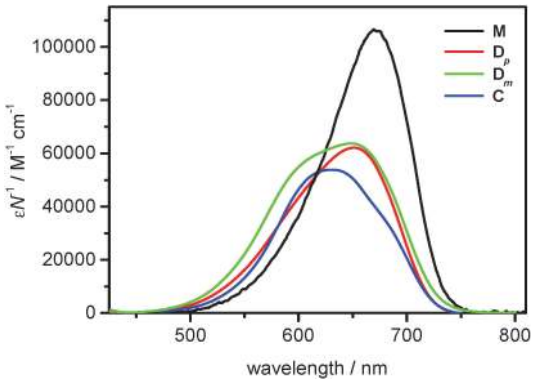

Fig. 3 Molar extinction coefficients measured in chloroform solutions, normalized with respect to the number of sub-chromophores, N.

interactions also influence the chemical reactivity as a result of strong repulsive electrostatic interactions that operate in the transition state involved in the last step of the formation of the dimers (leading to higher activation energy). As a further demonstration of this phenomenon, the yield of the cyclic dimer is even lower (13%), due to even stronger repulsive dipolar interactions in the transition state involving closure due to the close proximity which further increase the repulsion interactions, and subsequently the activation energy.

UV-Vis absorption characteristics of all the compounds in chloroform are summarized in Table 1, and absorption spectra normalized with respect to the number of chromophoric subunits are displayed in Fig. 3. All compounds exhibit strong absorption in the visible region. A net *hypsochromic* shift (19–40 nm; 510–950 cm^{-1}) as well as a definite *hypochromic* shift accompanied by a broadening towards the short-wavelength region, observed in the case of $\mathbf{D}_p$, $\mathbf{D}_m$ and **C**, clearly point to the existence of strong interchromophoric interactions within the dimers. The absorption band of dimers is characterized by two typical excitonic features, signature of excitonic coupling between the chromophoric subunits.[49–52] This effect is more pronounced the closer are the subchromophores in the dimers, emphasizing the role of confinement (*i.e.* increased through-space interactions between chromophoric subunits). Moreover, significant reduction of maximum values of the molar extinction coefficients per chromophoric subunit (ε^{max}/N) for the dimers (including for macrocycle **C**) as compared to that of monomer **M** (Fig. 3) provides further evidence that the chromophoric subunits do interact within the covalent dimers. This mutual interaction is thus responsible for improved transparency in most part of the spectrum (namely, at wavelengths longer than about 620 nm).

In order to gain further information on the effect of dipolar interactions on the polarisation of chromophoric subunits in dimers, ^{1}H NMR spectroscopy was conducted in chloroform both for monomer and dimers. In particular, the variation in the ^{1}H–^{1}H coupling constants ($^3J_{HH}$) along the polyenic chain of these push–pull systems was investigated to get information about the variation of BLA, which is correlated to the ground-state polarisation.[8] The coupling constants, $^3J_{HH}$, determined for the vicinal protons along the polyenic linker, and the resulting

difference in coupling constant values, ΔJ, are provided in Table 1. Although NMR studies are typically conducted at higher concentrations than UV-Vis spectroscopy (and thus contribution from *inter*molecular interactions cannot be excluded), we expect intramolecular electrostatic interactions within dimers to remain predominant as compared to intermolecular interactions. The observed variation of ΔJ values between the model monomer and the dimers (Table 1) hence suggests a notable variation of BLA. Indeed, when going from the monomer to the dimeric derivatives, ΔJ values increase indicating an increase in BLA values.[8] This suggests that the electrostatic interactions between the dipolar chromophoric subunits lead in this case to a *decrease of their polarisation* (*i.e.* increased contribution of the neutral form with respect to the zwitterionic form in the ground-state). This is consistent with the effect of the electric field generated by each dipolar subunit on the other subunit, due to their close proximity within the dimers (as illustrated in the picture sketched in Fig. 1).[53] Based on the evolution of the dipolar character of the subchromophores in dimeric compounds (getting closer to optimum BLA, *i.e.* 0.05 Å, and ΔJ = 3 Hz),[8] an enhancement of the hyperpolarisability of the constituting chromophoric subunits is thus anticipated.

In order to test this expectation, hyper-Rayleigh scattering (HRS) measurements were conducted in highly dilute chloroform solutions ($\approx 10^{-6}$ M) in order to avoid aggregation effects due to *inter*molecular interactions between polar molecules (monomer or dimers)[21,22] and single out the effects of through-space interactions *within* multimers. The experiments were performed at 1907 nm, away from two-photon resonance in order to avoid contamination of the HRS signal by fluorescence. HRS data for all the compounds are provided in Table 1. The first hyperpolarisability values of multichromophoric compounds are found to be non-zero and larger than that of the monomeric model compound, indicating that the push–pull chromophoric subunits self-orientate in a non-centrosymmetric fashion in the dimers and coherently contribute to the second-order nonlinear response. Moreover, the β_0^{HRS} (*i.e.* static) values were found to increase more rapidly than the number of chromophoric subunits, as illustrated in Fig. 4, top panel. Strikingly, an *enhancement of up to* 54% of the static hyperpolarizability response β_0^{HRS} *per chromophoric subunit* is recorded (Table 1). To our knowledge, this is the first time that such amplification, accompanied by an increase in transparency, is observed in non-rigid multichromophoric systems built from dipolar chromophores. Indeed, most of the time a reduction is observed.[21–23,25,26,28–33] In previous reports of β enhancement per subunit in multichromophoric or dimeric architectures, a red-shift of the ICT band and subsequent loss in transparency was always observed.[54,55] To our knowledge, this is the first time such a marked effect, driven only by through-space dipolar interactions within self-orientating multichromophoric architectures, is achieved.

In order to gain further insight into this phenomenon, we investigated the variation of the NLO response of each chromophoric subunit as a result of the mutual through-space interactions operating within dimers. Approximating the

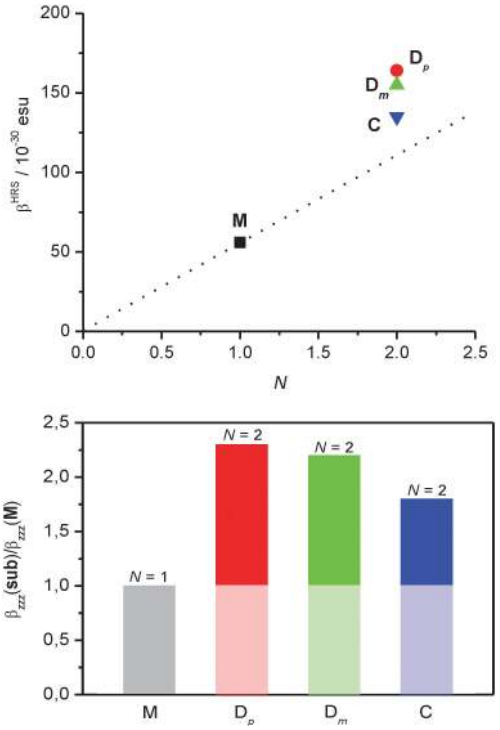

Fig. 4 (top) First hyperpolarisability (β^{HRS}) of the four compounds, measured in a chloroform solution, reported as a function of the number of subchromophores. (bottom) The β_{zzz}(**sub**)/β_{zzz}(**M**) ratio estimated for the four compounds.

push–pull units as one-dimensional chromophores with a dominant longitudinal component,[56] β_{zzz}, the β^{HRS} value for the monomer is given by:

$$\beta^{HRS}(\mathbf{M}) = \sqrt{\frac{6}{35}}\beta_{zzz}(\mathbf{M}) \quad (3)$$

Assuming a C_{2v} structure for the dimers (**D**), their β^{HRS} can be expressed as a function of the angle α (tilt angle with respect to the symmetry axis) and of the response of each of the chromophoric subunits, β_{zzz}(**sub**):[28]

$$\beta^{HRS}(\mathbf{D}) = 2\sqrt{\frac{6}{35}}F(\alpha)\beta_{zzz}(\mathbf{sub}) \quad (4)$$

with:

$$F(\alpha) = \sqrt{\cos^6\alpha + \frac{8}{9}\cos^4\alpha\sin^2\alpha + \frac{19}{9}\cos^2\alpha\sin^4\alpha} \quad (5)$$

Consequently the amplification factor β^{HRS}(**D**)/[2β^{HRS}(**M**)] can be expressed as:

$$\frac{\beta^{HRS}(\mathbf{D})}{2\beta^{HRS}(\mathbf{M})} = F(\alpha)\frac{\beta_{zzz}(\mathbf{sub})}{\beta_{zzz}(\mathbf{M})} \quad (6)$$

where the ratio β_{zzz}(**sub**)/β_{zzz}(**M**) allows us to estimate the *intrinsic* effect of through-space interactions on the NLO response of the chromophoric subunits, while $F(\alpha)$ only depends on the mutual orientation. Since $F(\alpha) \leq 1$ (see Fig. 2), the intrinsic enhancement factors (see Table 1) are even larger than the bare amplification

factors based on the β^{HRS} values. This clearly demonstrates that the *hyperpolarisability of the chromophoric subunits increases significantly* in the dimeric structures as a result of the change of polarity of the chromophoric subunits themselves (as evidenced by NMR studies) triggered by through-space dipolar interactions.

The results presented here can be further analysed by means of the theoretical model[47] summarized in the Experimental section, based on a two-level description of the push–pull chromophoric subunits (see ESI†). Only electrostatic interactions are taken into account between subunits, giving rise to the well-known excitonic term (exciton hopping), plus mean-field interaction, plus other contributions describing the exciton–exciton interaction and the interaction between states having a different exciton number.[46,47]

We optimized the two-state model parameters for the model monomer and the geometrical parameters for the dimers in order to be able to obtain a good description of the linear and nonlinear optical properties of the compounds. The best parameters are reported in Table 2, allowing the calculation of the absorption spectra shown in Fig. 5.

The spectra of the dimers can be well reproduced by fixing an interchromophore distance ranging from 8 to 8.5 Å and an angle (α, see sketch in Table 2) of about 50° for $\mathbf{D}_p$ and $\mathbf{D}_m$ and 35° for **C**. In the measured spectra (Fig. 5), the excitonic splitting is well apparent, accompanied by spectral broadening and lowering of the maximum values of molar extinction coefficients for dimers, in agreement with the experimental behaviour (see Fig. 3).

On the other side, static (hyper)polarisabilities are ground-state properties, so that a mean-field approach is enough for their description: this means that static hyperpolarisabilities can be obtained as successive finite-field derivatives of the ground-state dipole moment, provided the dipole moment is calculated in the mean-field approximation, *i.e.* readjusting this value in response to the electric field generated by the other interacting chromophore(s).[47] The same holds true for dynamic polarisabilities measured at a very low frequency, far away from any resonance. This suggests a unique way to explain an increase of the first hyperpolarisability per chromophoric subunit when going from the monomer to the dimers, staying consistent with a blue shift of the absorption band. In fact, the first hyperpolarisability of a push–pull molecule is a function of the charge-separation (or intramolecular charge transfer) degree in the ground state (ρ), being maximized for ρ values of about 0.3 (or 0.7 for molecules with mainly zwitterionic ground states, see Fig. 6).[16,17] We stress that this variation exactly parallels the well-known variation of the hyperpolarisability of push–pull polyenes as a function of BLA.[8,14]

The push–pull chromophore **M** does not have a zwitterionic character in its ground state, as indicated by its positive solvatochromic behaviour (see ESI†). An increase of the first hyperpolarisability per chromophoric subunit in the dimers, accompanied by a blue shift of the absorption band in response to the repulsive interaction with the other subunit, can only be justified by invoking a *decrease* of the charge-separation degree ρ (concomitant to an increase of BLA), from a value between 0.3 and 0.5 for the monomer to a value closer to 0.3 for the dimers. This is consistent with the increase of BLA when going from the monomer to the dimers ascertained by the experimental observation of increased ΔJ values by NMR spectroscopy. In fact, the BLA is expected to be maximized for ρ = 0 or 1, and have a minimum for ρ = 0.5 (the so-called cyanine limit). In particular, our modelling suggests ρ = 0.47 for the model chromophore and ρ = 0.43 for each of the two subchromophores in the

Table 2 Parameters used for the calculation of the spectroscopic responses of the monomer and the dimers. Right: sketch of the dimer structure

	η [eV]	$\sqrt{2}t$ [eV]	d [Å]	A [°]
M	0.06	0.92	—	—
$\mathbf{D}_p$	0.06	0.92	8.5	50
$\mathbf{D}_m$	0.06	0.92	8	50
C	0.06	0.92	8	35

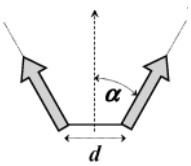

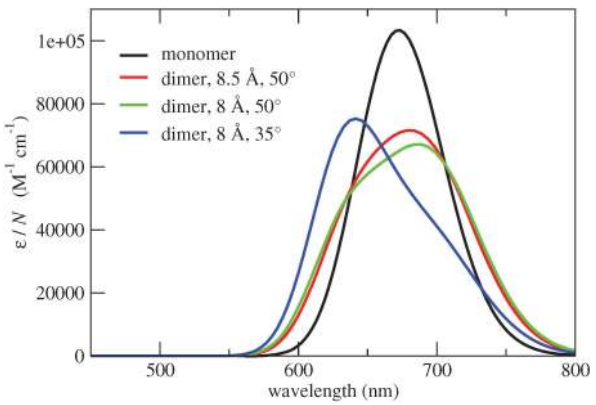

Fig. 5 Calculated absorption spectra (normalized for the number of subchromophoric units, N) for the monomeric model and for dimers of different geometry (as specified in the legend through d and α parameters, respectively). Parameters reported in Table 2, dipole moment of the zwitterionic basis state μ_0 = 21 D.

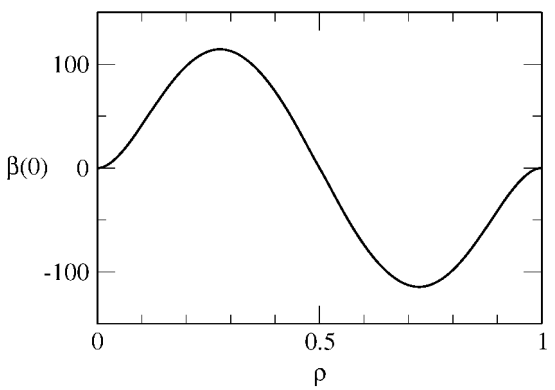

Fig. 6 Dependence of the static first hyperpolarizability, $\beta(0)$, on the degree of ground-state intramolecular charge transfer, ρ, for a push–pull chromophore described through a two-level model.

dimers. The fixed model parameters not only allow the reproduction of the absorption spectra of the monomer and dimers, but also the amplification of the HRS hyperpolarisability in dimers (see Table S1 in ESI†).

As pointed above, independently of the value of the interchromophoric angle, a $\beta^{HRS}(\mathbf{D})/[2\beta^{HRS}(\mathbf{M})]$ ratio greater than 1 unambiguously points to an amplification of the β_{zzz} response of each of the chromophoric subunits with respect to that of the isolated monomer. The estimation of the dimer geometry (in particular the interchromophore angle) given by the theoretical modelling allows us to estimate the real amplification of the first hyperpolarisability of the chromophoric subunits in the dimers with respect to the model monomer (*i.e.* $\beta_{zzz}(\mathbf{sub})/\beta_{zzz}(\mathbf{M})$). These values are estimated to amount to 2.3, 2.2 and 1.8 for $\mathbf{D}_p$, $\mathbf{D}_m$ and **C**, respectively (see Fig. 4, bottom panel). This implies an amplification of the β response of the chromophoric subunit in the dimers with respect to the monomer that we can safely estimate as high as ~100%. This result is even more striking given the blue-shift of the absorption band of the dimers with respect to the model chromophore, usually causing a lowering of the first hyperpolarisability per chromophoric subunit.[28–33] Interestingly, we observe that the effect seems to be more pronounced for the *para* and *meta* dimers as compared to the cyclic dimer. This indicates that the degree of freedom (controlled by covalent bonding) and distance between chromophoric subunits plays a subtle role in determining the amplitude of the cooperative effects due to the combination of mutual repulsion and polarisation effects. This emphasizes that fine tuning of the interactions by playing both on the nature of the chromophoric subunits (polarity, polarisability) and geometry of the dimeric architectures (distance, restricted freedom...) is a requisite for achieving cooperative enhancement of the NLO response. Indeed when the chromophoric subunits are too far apart and/or have lower polarity/polarisability,[57] only self-orientation is obtained without modification of the NLO response of each chromophoric subunit. The chromophoric subunits utilized in this work were designed on purpose as strongly polar and polarisable, as opposed to classical prototypical NLO chromophores (such as DANS or pNA type derivatives) mostly used in earlier multichromophoric architectures. This approach may be of interest for the incorporation of such cooperative multichromophoric systems into poled polymers for electro-optic (EO) modulation. In that respect, it is interesting to note that the dipole moments of the open dimers ($\mathbf{D}_m$ and $\mathbf{D}_p$) are expected to be only slightly larger than that of their monomer counterpart (while the cyclic dimer is only 50% larger), thanks to polarisation effects and to self-orientation of the subchromophores (see Table S1 in ESI†), thus opening the route for reduced intermolecular interactions (for a similar concentration in chromophoric subunits) and improved EO efficiency.

5 Conclusion

In summary, based on appropriate molecular design, synthesis and investigation of a set of related dimers and monomer, we have demonstrated that *electrostatic through-space interchromophoric interactions* can be exploited to achieve significant cooperative enhancement of second-order NLO responses while increasing transparency. This opens a new route for rational molecular engineering of NLO materials for electro-optic modulation by taking advantage of *intramolecular* dipolar interactions between close push–pull chromophores. Key ingredients are both the polarity and polarisability of the chromophoric subunits and the geometrical constraints imposed by covalent bonding which allow tuning of their mutual orientation and polarisation in a self-consistent way. Going one step further, the number of chromophoric subunits and the symmetry of the platform used for covalent bonding should also be considered.

Acknowledgements

MBD and PKD thank the Indo-French Centre for Promotion of Advanced Research (IFCPAR)/Centre Franco-Indien pour la Promotion de la Recherche Avancée (CEFIPRA) for financial support, and a PDF to VP. MBD gratefully acknowledges financial support from Conseil Régional d'Aquitaine (Chaire d'accueil grant).

References

1 P. A. Sullivan and L. R. Dalton, *Acc. Chem. Res.*, 2010, **43**, 10.
2 C. V. McLaughlin, L. M. Hayden, B. Polishak, S. Huang, J. Luo, T.-D. Kim and A. K.-Y. Jen, *Appl. Phys. Lett.*, 2008, **92**, 151107.
3 M. Lee, H. E. Katz, C. Erben, D. M. Gill, P. Gopalan, J. D. Heber and D. J. McGee, *Science*, 2002, **298**, 1401.
4 Y. Shi, C. Zhang, H. Zhang, J. H. Bechtel, L. R. Dalton, B. H. Robinson and W. H. Steier, *Science*, 2000, **288**, 119.
5 S. R. Marder, B. Kippelen, A. K.-Y. Jen and N. Peyghambarian, *Nature*, 1997, **388**, 845.
6 T. J. Marks and M. A. Ratner, *Angew. Chem., Int. Ed.*, 1995, **34**, 155.
7 D. M. Burland, R. D. Miller and C. A. Walsh, *Chem. Rev.*, 1994, **94**, 31.
8 M. Blanchard-Desce, V. Alain, P. V. Bedworth, S. R. Marder, A. Fort, C. Runser, M. Barzoukas, S. Lebus and R. Wortmann, *Chem. – Eur. J.*, 1997, **3**, 1091.
9 V. Alain, L. Thouin, M. Blanchard-Desce, U. Gubler, C. Bosshard, P. Günter, J. Muller, A. Fort and M. Barzoukas, *Adv. Mater.*, 1999, **11**, 1210.
10 J. Y. Lee, B. J. Mhin, S. Mukamel and K. S. Kim, *J. Chem. Phys.*, 2003, **119**, 7519.
11 A. Corozzi, B. Mennucci, R. Cammi and J. Tomasi, *J. Phys. Chem. A*, 2009, **113**, 14774.
12 F. Rizzo, M. Cavazzini, S. Righetto, F. De Angelis, S. Fantacci and S. Quici, *Eur. J. Org. Chem.*, 2010, 4004.
13 A. Plaquet, B. Champagne, J. Kulhanek, F. Bures, E. Bogdan, F. Castet, L. Ducasse and V. Rodriguez, *ChemPhysChem*, 2011, **12**, 3245.
14 S. R. Marder, L. T. Cheng, B. G. Tiemann, A. C. Friedli, M. Blanchard-Desce, J. W. Perry and J. Skindhoej, *Science*, 1994, **263**, 511.

15 L. R. Dalton, *J. Phys.: Condens. Matter*, 2003, **15**, R897.
16 M. Barzoukas, C. Runser, A. Fort and M. Blanchard-Desce, *Chem. Phys. Lett.*, 1996, **257**, 531.
17 A. Painelli, *Chem. Phys. Lett.*, 1998, **285**, 352.
18 R. Sen, D. Majumdar, K. K. Das and S. P. Bhattacharyya, *Indian J. Chem., Sect. A: Inorg., Bio-inorg., Phys., Theor. Anal. Chem.*, 2001, **40**, 804.
19 G. Archetti, A. Abbotto and R. Wortmann, *Chem. – Eur. J.*, 2006, **12**, 7151.
20 F. Terenziani, V. Parthasarathy, A. Pla-Quintana, T. Maishal, A.-M. Caminade, J.-P. Majoral and M. Blanchard-Desce, *Angew. Chem., Int. Ed.*, 2009, **48**, 8691.
21 F. Würthner, S. Yao, T. Debaerdemaeker and R. Wortmann, *J. Am. Chem. Soc.*, 2002, **124**, 9431.
22 F. Terenziani, S. Ghosh, A.-C. Robin, P. K. Das and M. Blanchard-Desce, *J. Phys. Chem. B*, 2008, **112**, 11498.
23 A. Lohr, M. Grüne and F. Würthner, *Chem. – Eur. J.*, 2009, **15**, 3691.
24 S. Di Bella, M. A. Ratner and T. J. Marks, *J. Am. Chem. Soc.*, 1992, **114**, 5842.
25 Y. Shi, C. Zhang, H. Zhang, J. H. Bechtel, L. R. Dalton, B. H. Robinson and W. H. Steier, *Science*, 2000, **288**, 119.
26 H. Ma and A. K.-Y. Jen, *Adv. Mater.*, 2001, **13**, 1201.
27 D. L. Elder, S. J. Benight, J. Song, B. H. Robinson and L. R. Dalton, *Chem. Mater.*, 2014, **26**, 872.
28 E. Kelderman, W. A. J. Starmans, J. P. M. van Duynhoven, W. Verboom, J. F. J. Engbersen, D. N. Reinhoudt, L. Derhaeg, T. Verbiest, K. Clays and A. Persoons, *Chem. Mater.*, 1994, **6**, 412.
29 H.-J. Deussen, E. Hendrickx, C. Boutton, D. Krog, K. Clays, K. Bechgaard, A. Persoons and T. Bjørnholm, *J. Am. Chem. Soc.*, 1996, **118**, 6841.
30 P. J. A. Kenis, O. F. J. Noordman, S. Houbrechts, G. J. van Hummel, S. Karkema, F. C. J. M. van Veggel, K. Clays, J. F. J. Engbersen, A. Persoons, N. F. van Hulst and D. N. Reinhoudt, *J. Am. Chem. Soc.*, 1998, **120**, 7875.
31 Y. Liao, K. A. Firestone, S. Bhattacharjee, J. Luo, M. Haller, S. Hau, C. A. Anderson, D. Lao, B. E. Eichinger, B. H. Robinson, P. J. Reid, A. K.-Y. Jen and L. R. Dalton, *J. Phys. Chem. B*, 2006, **110**, 5434.
32 E. D. Rekaï, J.-B. Baudin, L. Jullien, I. Ledoux, J. Zyss and M. Blanchard-Desce, *Chem. – Eur. J.*, 2001, **7**, 4395.
33 G. Hennrich, M. Murillo, P. Prados, H. Al-Saraierh, A. El-Dali, D. Thompson, J. Collins, P. Georghiou, A. Teshome, I. Asselberghs and K. Clays, *Chem. – Eur. J.*, 2007, **13**, 7753.
34 S. K. Srivastavaa, P. M. S. Chauhana and A. P. Bhaduria, *Synth. Commun.*, 1999, **29**, 2085.
35 J.-M. Raimundo, P. Blanchard, N. Gallego-Planas, N. Mercier, I. Ledoux-Rak, R. Hierle and J. Roncali, *J. Org. Chem.*, 2002, **67**, 205.
36 C. W. Spangler and R. K. McCoy, *Synth. Commun.*, 1988, **18**, 51.
37 E. C. Taylor and K. S. Hartke, *J. Am. Chem. Soc.*, 1959, **81**, 2452.
38 N. Bloembergen, *Am. J. Phys.*, 1967, **35**, 989.
39 D. V. Guerra and R. B. Kay, *J. Phys. B: At., Mol. Opt. Phys.*, 1993, **26**, 3975.
40 S. Ghosh, A. S. Ranjini, R. Pandey and P. K. Das, *Chem. Phys. Lett.*, 2009, **474**, 307.
41 M. A. Pauley, H.-W. Guan, C. H. Wang and A. K.-Y. Jen, *J. Chem. Phys.*, 1996, **104**, 7821.
42 T. Kodaira, A. Watanabe, O. Ito, M. Matsuda, K. Clays and A. Persoons, *J. Chem. Soc., Faraday Trans.*, 1997, **93**, 3039.
43 M. A. Pauley and C. H. Wang, *Rev. Sci. Instrum.*, 1999, **70**, 1277.
44 M. A. Pauley and C. H. Wang, *Chem. Phys. Lett.*, 1997, **280**, 544.
45 A. Willetts, J. E. Rice, D. M. Burland and D. P. Shelton, *J. Chem. Phys.*, 1992, **97**, 7590.
46 V. M. Agranovich and M. D. Galanin, *Electronic Excitation Energy Transfer in Condensed Matter*, North-Holland Publishing Company, 1982.
47 F. Terenziani and A. Painelli, *Phys. Rev. B: Condens. Matter Mater. Phys.*, 2003, **68**, 165405.
48 K. Clays, E. Hendrickx, T. Verbiest and A. Persoons, *Adv. Mater.*, 1998, **10**, 643.
49 L. Lu, R. J. Lachicotte, T. L. Penner, J. Perlstein and D. G. Whitten, *J. Am. Chem. Soc.*, 1999, **121**, 8146.
50 S. Zeena and K. George Thomas, *J. Am. Chem. Soc.*, 2001, **123**, 7859.
51 F. Würthner, S. Yao and U. Beginn, *Angew. Chem., Int. Ed.*, 2003, **42**, 3247.
52 A. Zitzler-Kunkel, M. R. Lenze, K. Meerholz and F. Würthner, *Chem. Sci.*, 2013, **4**, 2071.
53 The contribution from *inter*molecular interactions (leading to antiparallel aggregation as reported in ref. 52) would lead to increased polarisation instead and thus reduced ΔJ. This suggests that intramolecular interactions dominate.
54 S. Yokoyama, T. Nakahama, A. Otomo and S. Mashiko, *J. Am. Chem. Soc.*, 2000, **122**, 3174.
55 C.-Z. Zhang, C. Lu, J. Zhu, C.-Y. Wang, G.-Y. Lu, C.-S. Wang, D.-L. Wu, F. Liu and Y. Cui, *Chem. Mater.*, 2008, **20**, 4628.
56 This intramolecular charge transfer implies a partial transfer of an electron from the electron-donating part of the molecule (the amino group) to the electron-withdrawing part of the molecule (the one characterized by the three cyano groups and the phthalimide moiety). The mean direction of this transfer (*i.e.* the direction of the ground-to-excited state transition dipole moment) represents the z axis for our molecule, as it is standard for push–pull molecules.
57 F. Terenziani, O. Mongin, C. Katan, B. K. G. Bhatthula and M. Blanchard-Desce, *Chem. – Eur. J.*, 2006, **12**, 3089.